JOURNAL OF VIROLOGY, Aug. 2008, p. 8112–8123 Vol. 82, No. 16
0022-538X/08/$08.00+0 doi:10.1128/JVI.00837-08

Mouse Hepatitis Virus Type 2 Enters Cells through a Clathrin-Mediated Endocytic Pathway Independent of Eps15[▽]

Yinghui Pu and Xuming Zhang*

Department of Microbiology and Immunology, University of Arkansas for Medical Sciences, Little Rock, Arkansas 72205-7199

Received 18 April 2008/Accepted 4 June 2008

It has recently been shown that cell entry of mouse hepatitis virus type 2 (MHV-2) is mediated through endocytosis (Z. Qiu et al., J. Virol. 80:5768–5776, 2006). However, the molecular mechanism underlying MHV-2 entry is not known. Here we employed multiple chemical and molecular approaches to determine the molecular pathways for MHV-2 entry. Our results showed that MHV-2 gene expression and infectivity were significantly inhibited when cells were treated with chemical and physiologic blockers of the clathrin-mediated pathway, such as chlorpromazine and hypertonic sucrose medium. Furthermore, viral gene expression was significantly inhibited when cells were transfected with a small interfering RNA specific to the clathrin heavy chain. However, these treatments did not affect the infectivity and gene expression of MHV-A59, demonstrating the specificity of the inhibitions. In addition, overexpression of a dominant-negative mutant of caveolin 1 did not have any effect on MHV-2 infection, while it significantly blocked the caveolin-dependent uptake of cholera toxin subunit B. These results demonstrate that MHV-2 utilizes the clathrin- but not caveolin-mediated endocytic pathway for entry. Interestingly, when the cells transiently overexpressed a dominant-negative form (DIII) of Eps15, which is thought to be an essential component of the clathrin pathway, viral gene expression and infectivity were unaffected, although DIII expression blocked transferrin uptake and vesicular stomatitis virus infection, which are dependent on clathrin-mediated endocytosis. Thus, MHV-2 entry is mediated through clathrin-dependent but Eps15-independent endocytosis.

Infection of host cells by a virus is usually initiated by binding of virion surface proteins with a specific receptor(s) on the cell membrane, which leads to internalization of the virus into cells. Depending on the presence or absence of viral envelope and the features of the virion surface, the mode of internalization can vary significantly. For most if not all of the animal viruses, internalization or cell entry usually follows, or preferentially uses, one of the two pathways, directly from the plasma membrane or through endocytosis, although some viruses may use both pathways under different conditions. The best-characterized endocytic pathways include those acting via the clathrin-coated pit and vesicles, as for Semliki Forest virus (35), vesicular stomatitis virus (VSV) (37, 63), and influenza A virus (36), and those acting via the caveolin-mediated lipid raft, as for simian virus 40 (SV40) (1).

In clathrin-mediated endocytosis, clathrin is first recruited to the plasma membrane in response to receptor-mediated internalization signals, which then leads to the assembly of clathrin-coated pits (CCPs) at the cytoplasmic side of the cell membrane. Clathrin is composed of light chain and heavy chain and forms a unique structure called clathrin triskelion (26). During the assembly of CCPs, the adaptor protein 2 (AP-2) provides a bridge between receptors' cargo domain and the clathrin coat, which occurs through binding of the AP-50 (μ2) subunit of AP-2 to both the receptors' cargo domain and the clathrin β subunit (27). Once assembled, CCPs pinch off from the cell membrane and mature into clathrin-coated vesicles (26), which then deliver the cargo into endosomes. There are multiple cellular adaptors or accessory proteins interacting with each other and regulating this process. One of those regulatory proteins is Eps15, which was initially identified as the substrate of epidermal growth factor receptor (EGFR) and found to be constitutively associated with AP-2 (6). Microinjection of anti-Eps15 antibody interfered with transferrin and EGFR internalization, suggesting that Eps15 plays an important role in both constitutive and ligand-induced endocytic processes (9). Eps15 consists of three structural domains. The EH (Eps homolog) domain is located at the N terminus and regulates Eps15 binding to regulatory proteins that contain the Asn-Pro-Phe sequence, including Epsin, AP180, and synaptojanin (55). The central domain mediates the oligomerization of Eps15 (65), and the C-terminal domain contains repeats of the Asp-Pro-Phe sequence and the AP-2-binding site (7). Overexpression of the Eps15 C-terminal domain results in a dominant-negative effect that inhibits clathrin-mediated endocytosis. This dominant-negative protein also blocks infection with human polyomavirus JC virus (52) and Sindbis virus (9), which use clathrin-dependent endocytosis for entry. In general, during endocytosis, virus is first transported to early endosomes and then to late endosomes, where the vesicular microenvironment triggers conformational changes in viral proteins on the viral envelope or capsid and leads to penetration, the delivery of viral genomes into the cytoplasm.

In addition to clathrin-mediated endocytosis, another important entry pathway for animal viruses is mediated through lipid raft caveolae. The lipid rafts are high-curvature, cholesterol-rich membrane structures that are important in many biological events, such as endocytic traffic, signal transduction,

* Corresponding author. Mailing address: Department of Microbiology and Immunology, University of Arkansas for Medical Sciences, 4301 West Markham Street, Slot 511, Little Rock, AR 72205-7199. Phone: (501) 686-7415. Fax: (501) 686-5359. E-mail: zhangxuming@uams.edu.

[▽] Published ahead of print on 11 June 2008.

protein sorting, and membrane transport (8, 17). Caveolae are defined as specialized lipid raft domains with caveolins as the major integral membrane proteins. The invaginated caveolae are usually 50 to 70 nm in size and are abundant in many cell types (2). In mammals, there are three caveolin gene products, caveolins 1, 2, and 3, with a similar molecular weight of approximately 22 kDa (57, 64). Those 22-kDa caveolins tightly bind to cholesterol in the membrane through a 33-amino-acid hydrophobic domain, leaving the amino and carboxyl portions free in the cytoplasm and forming a striated coat (29, 53). Caveolins are well conserved in amniotes. The major differences among them are the posttranslational modification and tissue specificity. Caveolins 1 and 2 are expressed in most cell types and have similar tissue distributions, while caveolin 3 is present primarily in muscle cells (60). However, only caveolins 1 and 3 are essential for the formation of caveola invaginations (42, 44, 45). Recently lipid rafts, particularly the caveolae, have been shown to be an important entry route for many pathogens, including viruses and bacteria (4, 10, 13). The involvement of membrane rafts in entry of envelope viruses has been documented for several viruses, including influenza A virus, human immunodeficiency virus, murine leukemia virus, measles virus, and Ebola virus; all of their receptors are associated with membrane rafts (16, 33, 34, 50, 56). Caveola-mediated endocytosis has also been reported to be involved in human coronavirus 229E entry in human fibroblasts (43).

Mouse hepatitis virus (MHV) is a member of the *Coronaviridae*, a group of enveloped viruses with a positive-strand RNA genome. Depending on the viral strain, there are three to four proteins present in the envelope. The spike (S) protein is a type I membrane glycoprotein with a molecular mass of approximately 180 kDa. The S protein from several MHV strains can be cleaved by furin-like proteases into the amino-terminal subunit (S1) and the carboxyl-terminal subunit (S2). The extent of the cleavage also depends on the cell types in which the virus grows and affects virus-induced cell-to-cell fusion (19). Interestingly, the cleavability of the S protein may also control the route of virus entry. For example, the S protein of MHV type 2 (MHV-2) is usually not cleaved, and MHV-2 enters cells via the endocytic pathway (51). In contrast, a recombinant MHV, RA59/MHV-2$S_{S757R,}$ whose S protein has a single amino acid mutation relative to the MHV-2 S protein and is readily cleaved, likely enters cells through direct fusion with plasma membrane (51). Interaction between the MHV S protein and the receptor, a murine CEACAM (carcinoembryonic antigen cell adhesion molecular) receptor (71), on the cell surface is the first step in viral infection. Thus, the S protein plays a critical role in viral infectivity. In addition to the S protein, two other membrane proteins (M and E) are important for virion assembly, while the hemagglutinin-esterase protein, which is present only in some MHV strains, such as JHM, is not essential for viral infectivity but may play a role in pathogenesis in vivo (73, 74). The viral nucleocapsid (N) protein is a phosphoprotein of approximately 50 kDa (61). It is associated with the viral RNA genome in the nucleocapsid and is abundantly expressed in infected cells.

Recent studies on the severe acute respiratory syndrome coronavirus (SARS-CoV) have shown that the virion S protein is uncleaved and that SARS-CoV S protein-mediated pseudoretrovirus entry takes place via endocytosis (59). Further, the SARS-CoV S protein is cleaved in the endosome via cathepsins, which is required for viral infectivity (59). Although SARS-CoV S-protein-mediated entry into HepG2 and COS7 cells is dependent on clathrin-mediated endocytosis (25), its entry into Vero E6 cells is mediated through a clathrin- and caveolae-independent endocytic pathway (69). Using nonfusogenic MHV-2, Qiu et al. (51) showed that MHV-2 also enters L2 cells via endocytosis and that cleavage of the S protein by cathepsins in the endosome is required for its infectivity. However, the molecular events leading to endocytosis by MHV are unknown. Here we attempted to characterize the molecular events of coronavirus entry by using MHV-2 as a model system. We showed that MHV-2 entry involves clathrin- but not caveolin-mediated endocytosis. Using the dominant-negative mutant of Eps15, which blocks transferrin uptake and inhibits VSV infection, we unexpectedly found that MHV-2 entry does not depend on Eps15. Since Eps15 has been shown to be an essential component of the extended AP-2 complexes that are required for assembly and transport of clathrin-coated pits, our data indicate that unlike VSV, Sindbis virus, and influenza A virus, MHV-2 may utilize an unidentified clathrin-mediated pathway that is independent of Eps15. Thus, MHV-2 may provide a tool for identifying novel cellular components that are involved in clathrin-mediated endocytosis but are independent of Eps15.

MATERIALS AND METHODS

Virus, cells, antibodies, and reagents. The mouse astrocytoma DBT cells (22) were used for all experiments throughout this study. DBT cells were cultured in minimal essential medium containing 7.5% newborn calf serum (Gibco), 10% tryptose phosphate broth, and 1 mM of penicillin and streptomycin. MHV-2 and MHV-A59 were kindly provided by Michael Lai (University of Southern California Keck School of Medicine, Los Angeles). They have been propagated in DBT cells for more than 30 passages in our laboratory. In some instances, virions were semipurified through a 30% sucrose cushion by ultracentrifugation at 100,000 $\times$ *g* for 3 h at 4°C. Virus pellet was resuspended in phosphate-buffered saline (PBS). Virus titers were determined by plaque assay with DBT cells. VSV was kindly provided by Marie Chow (University of Arkansas for Medical Sciences [UAMS]) and was propagated in HeLa cells cultured with Dulbecco minimal essential medium containing 5% fetal bovine serum. The titer of virus was determined by plaque assay with BHK cells. Monoclonal antibodies specific to mouse clathrin heavy chain and β-actin were purchased from Sigma. Monoclonal antibodies specific to the MHV N protein and the VSV G protein were gifts from Stephen Stohlman (The Cleveland Clinic) and Marie Chow, respectively. The small interfering RNA (siRNA) specific to clathrin heavy chain (catalogue no. 16704) and Silencer Negative Control no. 1 siRNA were purchased from Ambion, Inc. Two Eps15 deletion constructs were gifts from A. Benmerah and A. Dautry-Varsat (Institut Pasteur, Paris, France). The deletion construct DIII is an Esp15 dominant-negative mutant, while DIIIΔ2, which has an additional deletion of the AP-2-binding site, serves as a nonfunctional control for DIII. Both are fused in-frame to the carboxyl terminus of the enhanced green fluorescence protein (EGFP) and are expressed in mammalian cells. Two caveolin-1 constructs were gifts from Marie Chow. N-terminally green fluorescent protein (GFP)-tagged caveolin 1 (GFP–cav-1) inhibits caveola-mediated entry of SV40, therefore functioning as dominant-negative caveolin 1 (dn cav-1) (47). The C-terminally GFP-tagged caveolin 1 (cav-1–GFP) behaves like wild-type caveolin 1 (wt cav-1) (47), thus serving as a transfection control for dn cav-1. Chlorpromazine, chloroquine, and bafilomycin A1 were purchased from Sigma. These reagents were prepared in dimethylsulfoxide (DMSO). The final working concentration of DMSO was approximately 1%. Alexa Fluor 594-conjugated transferrin and cholera toxin subunit B were purchased from Molecular Probes, Inc.

Treatment of cells with endocytosis inhibitors. For treatment with chloroquine, bafilomycin A1, and chlorpromazine, DBT cells were grown on six-well plates to confluence and were preincubated with 50 μM chloroquine, 100 nM bafilomycin A1, or 10 μg/ml chlorpromazine for 30 min at 37°C. Pretreated

cells were then infected with MHV at a multiplicity of infection (MOI) of 10 in the presence of the respective inhibitor. Cells treated with 1% DMSO were used as mock-treatment controls. For sucrose treatment, DBT cells were pretreated with hypertonic (400 mM) sucrose medium for 30 min, followed by virus infection. For each inhibitor treatment, cell viability was determined to be >90% by trypan blue exclusion assay. Following virus infection, the inhibitors were present in the culture medium throughout the experiments unless stated otherwise.

Western blot analysis. Viral protein synthesis was detected at various time points postinfection (p.i.) by Western blot analysis. Briefly, infected cells were harvested and lysed in strong lysis buffer (25 mM HEPES, pH 7.5, 0.5% sodium deoxycholate, 1% Triton X-100, 0.2% sodium dodecyl sulfate (SDS), 5 mM EDTA, 1 mM Na_3VO_4, 20 mM β-glycerophosphate, 50 mM NaF) containing protease inhibitor cocktail tablets (Roche). Cell lysates were sonicated for 10 s on ice, followed by centrifugation to pellet the cell debris. The protein concentration was measured using the Bio-Rad protein assay kit (Bio-Rad, CA). Cell lysates were boiled for 5 min and chilled on ice, and equal amounts of total proteins were loaded onto gels. Proteins were separated by 10% SDS-polyacrylamide gel electrophoresis and then transferred to a nitrocellulose membrane (MSI, Westborough, MA) for 2 h at 40 V in a transfer buffer (25 mM Tris, 200 mM glycine, 20% methanol, 0.02% SDS). After being blocked with 5% skim milk in Tris-buffered saline for 1 h at room temperature (RT), the membrane was washed three times in Tris-buffered saline containing 0.5% Tween 20 and immunoblotted with a primary antibody for 2 h at RT, followed by a secondary antibody conjugated with horseradish peroxidase (1:2,500 dilution) (Sigma) for 1 h at RT. The target protein was detected by using an enhanced-chemiluminescence reagent (GE Healthcare). The amount of each band was quantified by using the LabWorks software program (UVP, Inc.).

DNA and RNA transfection. For DNA transfection, the Lipofectamine 2000 reagent was used according to the manufacturer's instructions (Invitrogen). Briefly, DBT cells were seeded on slides in 24-well culture plates at a density of 2×10^5 cells per well for 1 day. About 2.4 μg of plasmid DNAs and 1.5 μl of the Lipofectamine 2000 reagent were diluted separately in 50 μl of serum-free Opti medium without antibiotics, mixed, and incubated at RT for 20 min. DBT cells were washed with PBS, and 500 μl of serum-free medium was added to each well of the cell culture. The DNA-lipofectamine mixture was then added to each well, and the cell culture plates were incubated at 37°C. For siRNA transfection, DBT cells were seeded on six-well culture plates at a density of 10^5 cells per well. After incubation for 24 h, approximately 100 pmol of siRNA was transfected according to the manufacturer's protocol (Ambion, Inc.).

Flow cytometric analysis and fluorescence sorting. For flow cytometric analysis, cells expressing the GFP (or EGFP) and/or viral proteins were fixed for 10 min with 2% formaldehyde-PBS. For detection of viral N protein, fixed cells were stained with an anti-N-protein-specific monoclonal antibody on ice for 30 min and phycoerythrin (PE)-conjugated anti-mouse immunoglobulin G for another 30 min. Stained cells were analyzed on a BD FacsCalibur cytometer using the WinMDI2.8 software program (BD Bioscience). At least 10,000 cells per sample were analyzed. For (E)GFP sorting, approximately 2×10^7 transfected cells were subjected to sorting by using FacsAria (BD Bioscience). Cells giving medium to high green fluorescence intensity were collected as (E)GFP-positive cell populations, while cells not showing green fluorescence were collected as (E)GFP-negative cell populations.

Transferrin and cholera toxin subunit B uptake assays. For the transferrin uptake assay, DBT cells were washed and serum starved for 30 min, followed by incubation for 20 min in serum-free medium containing 50 μg/ml of Alexa Fluor 594-conjugated transferrin at 4°C. Cells were then washed with PBS and shifted to 37°C for 15 min. After that, 0.1 M glycine (pH 3.0) was used to wash away uninternalized transferrin on the cell membrane. Finally, cells were fixed in 2% paraformaldehyde and observed with a Zeiss Axioskop 2 deconvolution microscope. Images were captured by an AxioCam MRc color camera using AvioVision software. For the cholera toxin subunit B uptake assay, DBT cells were incubated with 5 μg/ml Alexa Fluor 594-conjugated cholera toxin subunit B (CT-B) for 30 min at 37°C, washed five times with culture medium, and then fixed with precooled (−80°C) methanol-acetone (32). Fluorescently labeled cells were visualized with a fluorescence microscope (Olympus IX-70), and photographs were taken with the attached digital camera (MagnaFire).

Statistical analysis. Where possible, data were analyzed for statistical significance and were expressed as means ± standard deviations. The mean values were compared using Student's *t* test. *P* values of <0.01 or <0.05 were considered statistically significant.

RESULTS

MHV-2 infection in DBT cells was impaired by inhibition of endosomal acidification. Although a recent study demonstrated that MHV-2 spike protein-mediated entry is sensitive to treatment with lysosomotropic agents in L2 cells (51), it has also been shown previously that different cell types have different abilities to cleave MHV spike protein and affect viral entry (19). In addition, the same MHV strain adapted in different laboratories with different passage histories and culture systems may have altered biological and pathogenic properties. Thus, to further dissect the entry pathway, it is essential to firmly establish whether the entry of our MHV-2 strain into DBT cells is also mediated via low-pH-dependent endocytosis. We used MHV-A59 as a control throughout this study because entry of MHV-A59 into DBT cells is independent of low pH. For this purpose, we used two lysosomotropic agents to pretreat DBT cells. Chloroquine is a weak base, and bafilomycin A1 is an inhibitor of the vacuolar proton pump ATPase, both of which can raise the pH in the endosomes and block virus entry via low-pH-dependent endocytosis. DBT cells were pretreated for 0.5 h with chloroquine (50 mM) or bafilomycin A1 (100 nM) or with DMSO (1%) as a control. Cells were then infected with MHV-2 or MHV-A59 at an MOI of 10 in the presence of the drugs. Titers of virus were determined by plaque assay at 7 h p.i., and viral gene expression was monitored by Western blot analysis from 5 to 7 h p.i. As shown in Fig. 1A, MHV-2 titers in drug-treated DBT cells were approximately 2 $\log_{10}$ lower than those in mock-treated cells at 7 h p.i. In contrast, MHV-A59 titers were unaffected by these lysosomotropic agents. Similarly, MHV-2 N-protein expression was significantly delayed in chloroquine-treated cells, compared with that in mock-treated cells (Fig. 1B and C), from 5 to 7 h p.i. ($P < 0.01$), while the expression of the MHV-A59 N protein was not affected by the drugs compared with that for the mock-treated controls ($P > 0.05$) (Fig. 1D and E). These results demonstrate that treatment with chloroquine and bafilomycin A1 suppressed MHV-2 but not MHV-A59 propagation, confirming that entry by our MHV-2 into DBT cells is mediated via pH-dependent endocytosis and that MHV-A59 entry is independent of low-pH conditions. These results also indicate that their inhibitory effects on MHV-2 are specific and are not due to the general cytotoxicity of the drugs since they did not have any inhibitory effect on MHV-A59 infection.

MHV-2 enters cells via clathrin-mediated endocytosis. It has been well established that cell entry of viruses via endocytosis can occur either dependently or independently of clathrin. To determine whether the endocytic entry pathway utilized by MHV-2 involves clathrin, several complementary approaches were employed. One approach was to use various inhibitors of the clathrin-mediated endocytosis. Chlorpromazine, which inhibits the recycling of AP2 between membranes and thus causes clathrin lattices to assemble on endosomal membranes and prevents coated pit assembly at the cell surface, was used to treat DBT cells at a concentration of 10 μg/ml for 30 min prior to virus infection. Cells were then infected with MHV-2 or MHV-A59 at an MOI of 10. Titers of virus in the medium were determined at 7 h p.i. Cell lysates were harvested at various time points p.i., and viral N-protein synthesis was analyzed as a readout of viral infection by Western blotting using

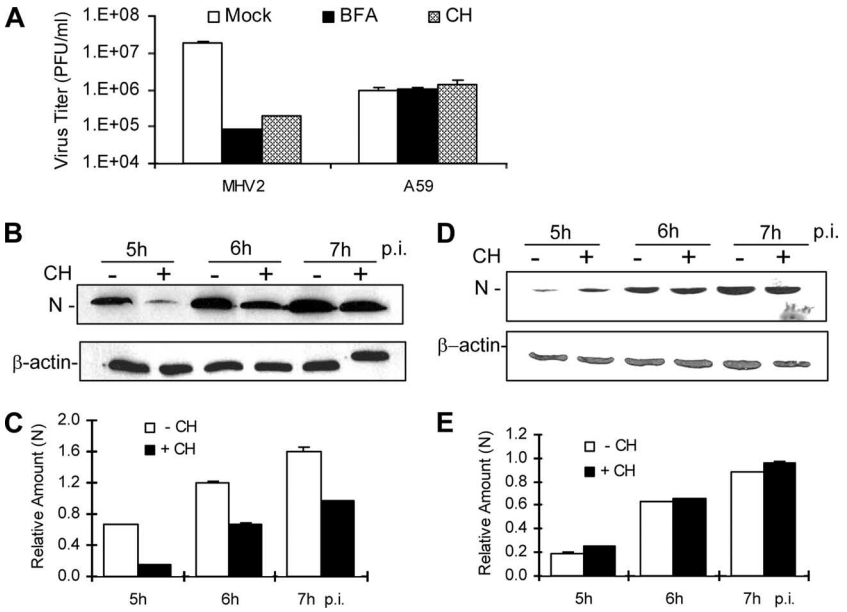

FIG. 1. MHV-2 infection was impaired by inhibition of endosomal acidification. (A) DBT cells were pretreated with chloroquine (50 μM) (CH), bafilomycin A1 (100 nM) (BFA), or DMSO (Mock) for 0.5 h prior to infection. Cells were infected with MHV-2 (MHV2) or MHV-A59 (A59) at an MOI of 10. Chloroquine or bafilomycin A1 was present in the medium throughout the infection. At 7 h p.i., titers of virus were determined by plaque assay and were expressed as mean PFU/ml from one of the three triplicate experiments. Error bars indicate standard deviations of the means. (B to E) MHV-2 gene expression was inhibited by chloroquine. DBT cells were treated with chloroquine and infected with MHV-2 (B) or MHV-A59 (D) as described for panel A. At the indicated time points p.i., infected cells were collected and viral N protein was detected with Western blot analysis. β-Actin was used as an internal control for normalization. The amount of each protein band was quantified by densitometric analysis with UPV software. The amount of N protein was normalized to β-actin expressed in virus-infected cells and is presented as a relative amount in panels C and E for MHV-2 and MHV-A59, respectively. Error bars indicate standard deviations of the means. Data are representative of three independent experiments.

an N-specific monoclonal antibody. As shown in Fig. 2A, the titer of MHV-2 was severely inhibited (≈3 $\log_{10}$ reduction) by chlorpromazine treatment compared with that of the mock-treated control. In contrast, the titer of MHV-A59 was only slightly reduced (<20%) under the same condition. Accordingly, the viral N-gene expression of MHV-2 was significantly inhibited in chlorpromazine-treated cells compared with that for mock-treated controls ($P < 0.01$) (Fig. 2B and C). These results indicate that MHV-2 entry into DBT cells likely depends largely on clathrin-mediated endocytosis, which appears, however, to play a minimal role if any in MHV-A59 entry. To confirm the above results, we employed a physiological method, i.e., use of hypertonic medium, to interfere with the clathrin pathway (21). When DBT cells were treated with a hypertonic medium, which contains sucrose at a concentration of 400 mM, before and during virus infection, the synthesis of the MHV-2 N protein was significantly delayed, from 5 to 7 h p.i. compared with that for mock-treated controls ($P < 0.01$) (Fig. 3A and B). By contrast, the levels of the MHV-A59 N protein synthesized during the same period were virtually identical in the presence or absence of the hypertonic sucrose medium ($P > 0.05$) (Fig. 3C and D).

As an alternative approach to explore the potential functions of clathrin in MHV-2 infection, we examined the effect of cytoskeleton network-modifying agents on MHV-2 infection. Clathrin-mediated endocytosis is usually coordinated with actin dynamics; therefore, destruction of the actin network by cytochalasin D inhibits clathrin-mediated endocytosis (14, 31, 39, 72). By contrast, caveolae have been shown to constitute a stationary structure in different cells lines (66). Ligand-induced signals trigger the transient recruitment of dynamin, a burst of actin polymerization to form an actin tail, and the internalization of caveola clusters (48). After pinching off from the plasma surface, caveolae move along the microtubule network to the destination (46). When the microtubule network is depolymerized by nocodazole, the ligand-induced internalization of a caveola cluster disappears (67). Therefore, we treated DBT cells with 4 μg/ml cytochalasin D, a potent inhibitor of actin microfilaments (40), or 4 μg/ml nocodazole, a potent microtubule disassembling agent (24). Mock-treated cells were used as controls. Inhibitor- or mock-treated cells were then infected with either MHV-2 or MHV-A59 at an MOI of 10. At various time points (5 to 7 h) p.i., a significant reduction of viral N-protein expression was observed for MHV-2 in cytochalasin D-treated cells but no significant reduction was found in nocodazole-treated cells compared to expression in mock-treated cells (Fig. 4A). By contrast, there was only a slight but insignificant reduction in viral N-protein synthesis for MHV-A59 in cytochalasin D-treated cells, and there was no effect from nocodazole treatment compared to synthesis in mock-treated cells (Fig. 4D, quantitative and statistical data not shown). The ability of the inhibitors to inhibit MHV-2 propagation was further tested at three different concentrations (4, 8, and 16 μg/ml for nocodazole and 1, 2, and 4 μg/ml for cytochalasin D) and monitored by determining virus titers. As shown in Fig. 4B, nocodazole had no significant effect on

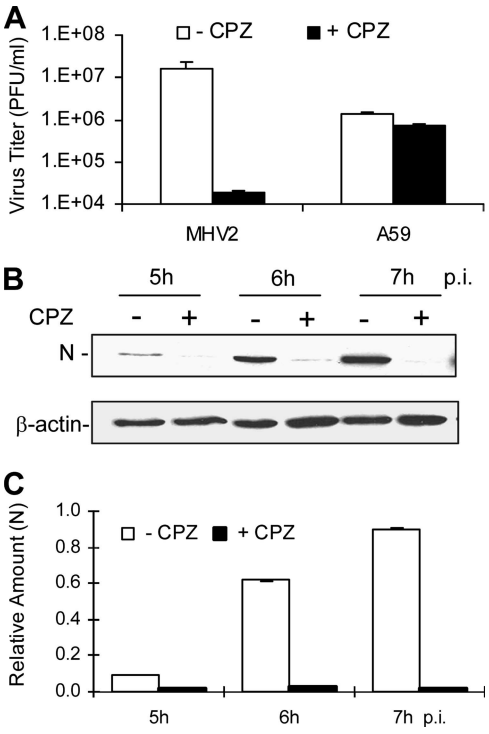

FIG. 2. Suppression of MHV-2 propagation by treatment with chlorpromazine (CPZ). (A) DBT cells were pretreated with chlorpromazine (10 μg/ml) for 0.5 h, followed by infection with MHV-2 or MHV-A59 (A59) at an MOI of 10. Chlorpromazine was kept in the medium throughout the infection (+ CPZ). Mock-treated cells were used as a negative control (− CPZ). The virus titer was determined at 7 h p.i. by plaque assay and expressed in mean PFU/ml from one of the three triplicate experiments. Error bars indicate the standard deviations of the means. (B) Chlorpromazine-treated (+) or mock-treated (−) cells were infected with MHV-2 at an MOI of 10. Infected cells were collected at the indicated time points p.i., and the viral N protein was detected with Western blot analysis using β-actin as an internal control for normalization. (C) Quantification of protein bands shown in panel B. The amount of each protein band was quantified by densitometric analysis with UPV software. The amount of N protein was normalized to β-actin expressed in virus-infected cells and is presented as a relative amount. Error bars indicate standard deviations of the means. Data are representative of at least three independent experiments.

titers of MHV-2 at any of the three concentrations. Interestingly, a significant reduction in the virus titer was observed only for MHV-2 in cytochalasin D-treated cells and only when cytochalasin D was added 30 min prior to virus infection ($P < 0.05$). When cytochalasin D was added 2 h p.i., it no longer had an inhibitory effect on the virus titer ($P > 0.05$) (Fig. 4C). In addition, the inhibitory effect of cytochalasin D on the MHV-2 titer was dose dependent, suggesting a specific inhibition. By contrast, regardless of whether the inhibitors were added 30 min prior to virus infection or 2 h p.i., neither nocodazole nor cytochalasin D had any significant effect on the titer of MHV-A59 ($P > 0.05$) (Fig. 4E and F, respectively). Taken together, these results demonstrate that blocking the clathrin-mediated endocytic pathway by either chemical agents or physiological methods affects MHV-2 infection in DBT cells, suggesting that clathrin-mediated endocytosis is involved in the early stages of the MHV-2 life cycle.

To provide direct evidence that MHV-2 uses the clathrin-mediated endocytic pathway for productive infection, we used siRNAs to specifically knock down the expression of clathrin heavy chain. We first examined whether clathrin expression was affected by siRNA transfection. At 48 h posttransfection, we found that transfection of siRNA indeed reduced clathrin expression to approximately 50% of that in the control siRNA-treated samples (Fig. 5A and B). When siRNA-transfected cells were infected with MHV-2 and examined by Western blotting for the synthesis of the viral N protein from 5 to 7 h p.i., again we observed a modest but statistically significant delay in DBT cells treated with the clathrin heavy-chain-specific siRNA compared with results for in the cells transfected with the nonspecific siRNA control ($P < 0.05$) (Fig. 5C and D). However, no reduction of N-protein expression for MHV-A59 was detected in cells transfected with the same clathrin heavy-chain siRNA ($P > 0.05$) (Fig. 5E and F). These results further confirm that the clathrin-mediated endocytic pathway is utilized by MHV-2 but not by MHV-A59 for its entry into DBT cells.

Caveolin-mediated lipid rafts are likely not involved in entry of MHV-2. The second well-characterized endocytic pathway is the clathrin-independent and caveolin-mediated lipid-raft-de-

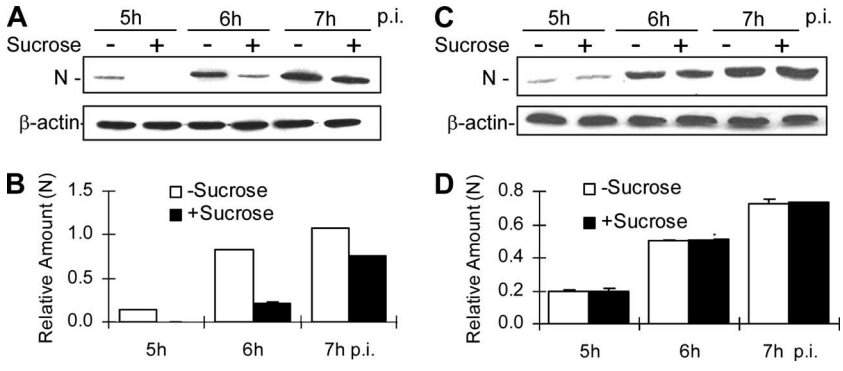

FIG. 3. MHV-2 propagation was impaired by hypertonic sucrose treatment. (A and C) DBT cells were pretreated with hypertonic (400 mM) sucrose (+) medium or mock-treated (-) for 0.5 h, followed by infection with MHV-2 (A) or MHV-A59 (C) at an MOI of 10. Expression of viral N protein was detected at various time points p.i. by Western blot analysis, with β-actin as an internal control for normalization. (B and D) Quantification of the protein bands shown in panels A and C, respectively. The amount of the N protein was quantified by densitometric analysis with UPV software, normalized with β-actin expressed in virus-infected cells, and presented as a relative amount. All data are representative of three independent experiments.

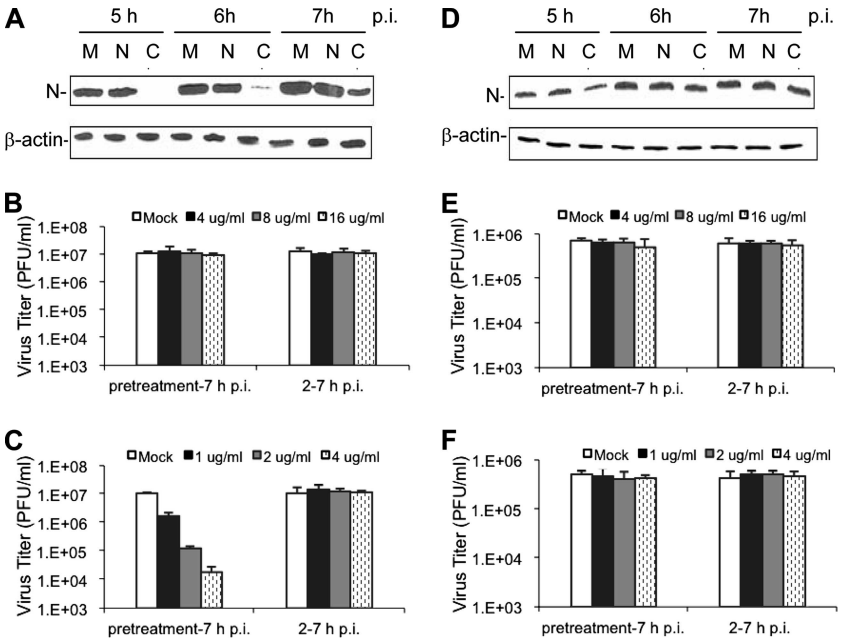

FIG. 4. Inhibition of MHV-2 infection by the actin cytoskeleton-modifying agent. (A and D) DBT cells were pretreated with nocodazole (N) or cytochalasin D (C) at 4 μg/ml or with DMSO as a mock control (M) for 0.5 h and then infected with MHV-2 (A) or MHV-A59 (D) at an MOI of 10. The drugs were kept in the medium throughout the infection. At the indicated time points p.i., viral N protein was determined by Western blotting, with β-actin as an internal control. (B, C, E, and F) DBT cells were treated with nocodazole (B and E) or cytochalasin D (C and F) either 0.5 h prior to infection (pretreatment-7 h p.i.) or 2 h after infection (2–7 h p.i.) at various concentrations (μg/ml) as indicated or treated with DMSO (Mock). DBT cells were infected with MHV-2 (B and C) or MHV-A59 (E and F) at an MOI of 10. Virus titers in the medium were determined at 7 h p.i. by plaque assay. The data are representative of three independent experiments and are indicated as mean PFU/ml from a triplicate experiment. Error bars indicate standard deviations of the means.

pendent pathway, as shown for SV40 entry (1). To determine whether MHV-2 can utilize more than one entry pathway, we analyzed the role of caveolin in viral entry. We expressed in DBT cells the dominant-negative mutant of caveolin 1 in which GFP is fused to the N terminus (GFP–cav-1) and determined whether the expression of the dominant-negative mutant of caveolin 1 inhibits MHV infection. At 48 h posttransfection, cells were subjected to fluorescence-activated cell sorting (FACS) to separate GFP–cav-1-expressing cells from nonexpressing cells. Both cell populations were then infected with MHV-2 at an MOI of 10. At 5 and 6 h p.i., cells were lysed and viral N proteins were detected with Western blotting. The results showed that there was no significant difference in virus infection in cells with or without the expression of the dominant-negative caveolin 1 (Fig. 6A and B). By contrast, the internalization of cholera toxin subunit B, which involves caveolin-mediated lipid rafts and which was used as a positive control, was significantly inhibited by the expression of the dominant-negative mutant of caveolin 1, while the expression of the wt cav-1 failed to block cholera toxin subunit B uptake, indicating the functional specificity of dominant-negative caveolin 1 (Fig. 6C). Combined with the results shown in Fig. 4, these data demonstrate that MHV-2 entry into DBT cells does not require caveolin-mediated lipid rafts.

Clathrin-mediated entry of MHV-2 is independent of Eps15. Eps15 has been characterized as being ubiquitously and constitutively associated with the AP-2 adaptor protein, and therefore it is thought to be an essential component of the clathrin-mediated endocytic pathway. It has been described previously that the expression of a dominant-negative form of Eps15, DIII, which contains the AP2-binding site of Eps15, could efficiently block the uptake of a cellular ligand, such as transferrin or epidermal growth factor, in HeLa cells, while another DNA construct (DIIIΔ2), with a deletion of the AP2-binding site based on the DIII construct, maintains the ability of transfected cells to uptake transferrin and thus serves as a negative control (6). To determine whether MHV-2 entry depends on Eps15, we used these constructs for transfection experiments. The GFP-tagged versions of DIII (EGFP-DIII) and DIIIΔ2 (EGFP-DIIIΔ2) were transiently expressed in DBT cells. These cells were then infected with MHV-2 at an MOI of 10 for 6 h, subjected to indirect immunofluorescence staining for the viral N protein with PE (red), and analyzed by FACS. To our surprise, expression of EGFP-DIII had no effect on the susceptibility of the cells to virus infection. As shown in Fig. 7A, under these experimental conditions, approximately 48% of the mock-transfected and virus-infected cells showed positive N staining whereas 31% of the EGFP-DIII-transfected and mock-infected cells showed an EGFP signal. Approximately 17% of cells were doubly positive for EGFP-DIIIΔ2 and virus infection. However, a similar number of cells doubly positive for EGFP and PE (17%) were detected in EGFP-DIII-transfected and virus-infected cells, suggesting that MHV-2 infection does not require Eps15.

To rule out the possibility that DIII could not act as a dominant-negative protein in our culture system, we then determined whether transferrin uptake, which is a marker for clathrin-mediated endocytosis, could be blocked by the Eps15

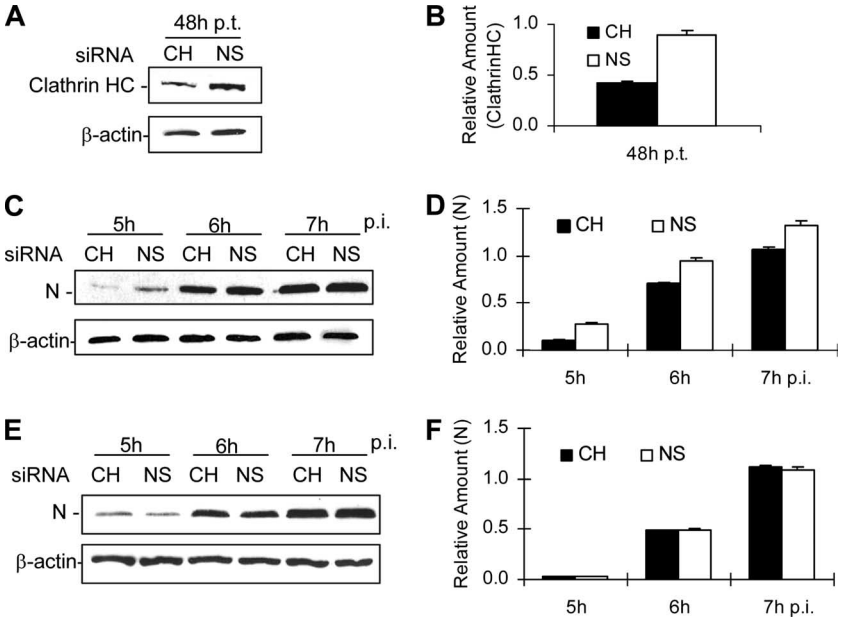

FIG. 5. Inhibition of MHV-2 propagation by siRNA specific to clathrin heavy chain. (A) DBT cells were transfected with either siRNA specific to clathrin heavy chain (CH) or a negative, nonspecific control siRNA (NS). At 48 h posttransfection (p.t.), cells were lysed and the protein level for the endogenous clathrin heavy chain (HC) was detected by Western blotting with an antibody specific to the clathrin heavy chain. The level for β-actin detected was used as an internal control for normalization. (B) Quantification of the protein bands shown in panel A. The amounts of the clathrin heavy chain were quantified by densitometric analysis, normalized to those of β-actin, and expressed as relative amounts. (C and F) Following transfection with either CH siRNA or NS siRNA for 48 h as shown in panel A, cells were infected with MHV-2 (C) or MHV-A59 (E) at an MOI of 10. At various time points p.i., as indicated, cells were collected and the expression of viral N protein was detected by Western blot analysis with β-actin as an internal control for normalization. (D and F) Quantification of the viral N protein shown in panels C and E, respectively. The methods used for quantification were identical to those described for panel B. The differences in N protein expression between specific (CH) and nonspecific (NS) siRNA-transfected cells were statistically significant ($P < 0.01$) in MHV-2-infected cells (D) but were not significant ($P > 0.05$) in MHV-A59-infected cells. The data are representative of three independent experiments.

dominant-negative mutant in DBT cells. Transfected cells were serum starved for 30 min, and Alexa Fluor 594-conjugated transferrin was added and incubated at 4°C to synchronize the binding. After cell cultures were shifted to 37°C for 15 min, glycine was used to wash away uninternalized transferrin. Expression of EGFP-DIII resulted in a pronounced inhibition of transferrin internalization, whereas in control cells that expressed EGFP-DIIIΔ2, transferrin was internalized normally (Fig. 7B). To further confirm the functional specificity of dominant-negative Eps15, we used VSV as a positive control in addition to transferrin, because it is well established that VSV enters cells via clathrin-mediated and Eps15-dependent endocytosis (63). As expected, expression of EGFP-DIII significantly inhibited viral G protein expression ($P < 0.01$) (Fig. 7C and D). These control experiments indicate that EGFP-DIII indeed functions as a dominant-negative inhibitor of Eps15 and that it affects clathrin-mediated endocytosis in our culture system.

As an alternative approach to verify this observation, cells transfected with EGFP-DIII were separated into EGFP-positive and EGFP-negative populations by cell sorting and were then infected with MHV-2 at an MOI of 10. The viral N-protein synthesis and viral titers were determined at various time points as appropriate. Consistent with the fluorescence staining, no significant difference in the kinetics of the N-protein synthesis was found between the two cell populations, as was the case with the viral titers ($P > 0.05$) (Fig. 8). Taken together, these results demonstrate that the dominant-negative mutant of Eps15, although it blocked transferrin uptake and VSV infection in DBT cells, failed to interfere with MHV-2 infection, suggesting that MHV-2 entry is independent of Eps15 for productive infection.

DISCUSSION

Recently it has been shown that MHV-2 enters fibroblast L2 cells through low-pH-dependent endocytosis (51). However, the molecular mechanisms underlying MHV-2 entry are unknown. In the present study, we employed chemical, physiological, and molecular approaches to characterize MHV-2 entry pathways in a mouse astrocytoma cell line, DBT, which has been extensively used for MHV propagation. Our results confirmed and extended the findings reported by Qiu et al. (51) that MHV-2 entry into DBT cells is also mediated via low-pH-dependent endocytosis (Fig. 1). Although endocytosis can involve either clathrin or caveolae, the low-pH dependency suggests that MHV-2 entry most likely utilizes the clathrin-mediated endocytosis pathway, since clathrin-mediated endocytosis usually requires an acidic environment in the endosome to induce the conformational changes in viral structure protein(s) (49). Furthermore, the results from dominant-negative caveolin 1 clearly exclude the involvement of caveola-mediated endocytosis in MHV-2 entry (Fig. 6). Our finding that the pharmacologic agent chlorpromazine significantly inhibited

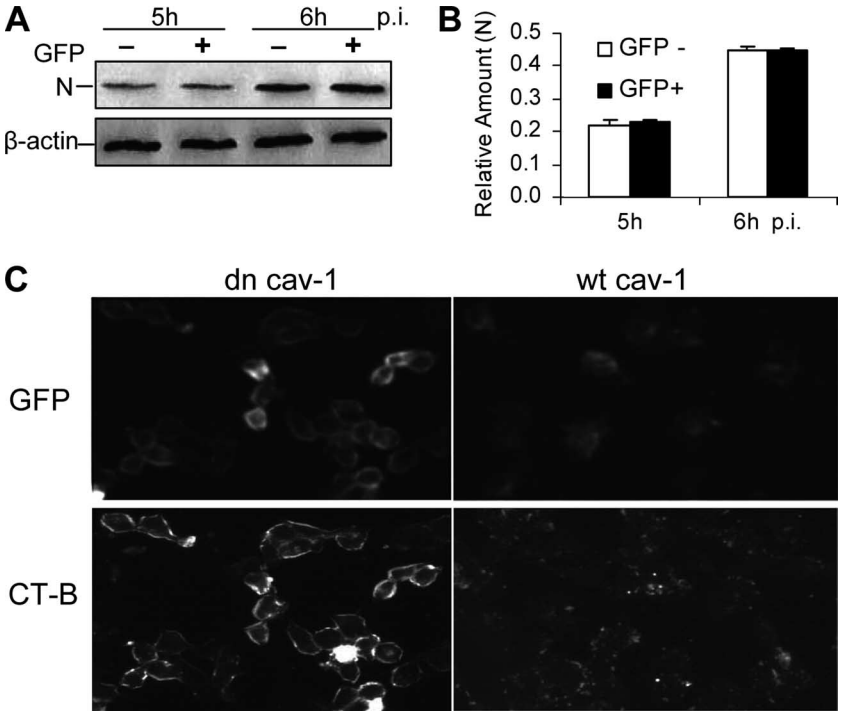

FIG. 6. Overexpression of a dominant-negative mutant of caveolin 1 could not suppress MHV-2 infection. (A) Effect of dominant-negative caveolin 1 on MHV-2 infection. DBT cells were transfected with GFP–cav-1 (dn cav-1). At 24 h posttransfection, DBT cells were subjected to FACS to separate GFP-positive (+) and GFP-negative (−) cell populations, which were then separately infected with MHV-2 at an MOI of 10. Expression of the viral N protein was detected by Western blot analysis, with β-actin as an internal control. (B) Quantification of the protein bands shown in panel A. The amounts of the N protein were quantified by densitometric analysis, normalized to those of β-actin, and expressed as relative amounts. (C) Effect of dominant-negative caveolin 1 on cholera toxin subunit B (CT-B) uptake. DBT cells were transfected with GFP–cav-1 (dn cav-1) or cav-1–GFP (wt cav-1). At 24 h posttransfection, cells were incubated with Alexa Fluor 594-conjugated CT-B for 30 min, washed, and fixed in precooled (−80°C) methanol-acetone. The images were taken with an Olympus IX-70 microscope and a digital camera (MagnaFire). Note that detection of GFP in the cells indicates the expression of the caveolin 1 plasmids, while detection of conjugated CT-B at the cell surface indicates the blockage of internalization.

MHV-2 infection supports the notion that MHV-2 enters DBT cells via clathrin-mediated endocytosis (Fig. 2), because chlorpromazine blocks the assembly of the clathrin-coated pits by blocking the recycling of AP-2 between the plasma membrane and the endosome (62, 70). It is worth noting that the inhibitory effect of chlorpromazine on viral infection was the greatest when it was present during the first hour of infection, suggesting that chlorpromazine likely acts on viral entry (data not shown). Consistent with this finding is the result from additional experiments with sucrose treatments and cytoskeleton modifying agents (Fig. 3 and 4). Although the mechanism of action for the inhibitory effect of hypertonic medium on clathrin-mediated endocytosis is still unclear, it has been well established that this treatment did disassemble the clathrin-coated pits and inhibit transferrin endocytosis (21). It also has been used to investigate the role of clathrin-mediated endocytosis in porcine circovirus-2 infection (41). The involvement of actin cytoskeleton in clathrin-mediated endocytosis was also well documented (14, 31, 39, 72). Although these chemical and physiological inhibitors may have other, nonspecific effects on viruses and cells, their failure to inhibit a closely related strain, MHV-A59, under the same conditions indicates that their inhibitory effects on MHV-2 are specific. In addition, we used an siRNA specific to the clathrin heavy chain to treat cells prior to viral infection. Compared to the clathrin light chain, the clathrin heavy chain is the essential component of the clathrin triskelion and is ubiquitously expressed in all cell types (68). Therefore, knockdown of heavy-chain expression can inhibit the function of clathrin-mediated endocytosis. This approach has also previously been used to examine the role of clathrin in adenovirus endocytosis (38). Although the clathrin heavy chain is expressed abundantly in DBT cells, transfection of the siRNA did specifically reduce its expression by approximately 50% at 48 h posttransfection. Even with such a low level of knockdown, we consistently observed a specific inhibition of MHV-2 gene expression following infection (Fig. 5). Taken together, our complementary approaches demonstrate that MHV-2 enters DBT cells via clathrin-mediated endocytosis while MHV-A59 likely utilizes a clathrin-independent pathway for entry.

It is important to note that previous studies have shown that cell entry of MHV-A59 is sensitive to lysosomotropic agents (ammonium chloride and bafilomycin A1) and is likely facilitated through the clathrin-mediated endocytic pathway (sensitive to chlorpromazine treatment) (12, 15). However, it has also been shown that MHV-A59 infection is insensitive to lysosomotropic agents such as ammonium chloride and bafilomycin A1 (51), which is similar to the results from our present study. One possible explanation for this apparent discrepancy is that MHV-A59 used in different laboratories around the

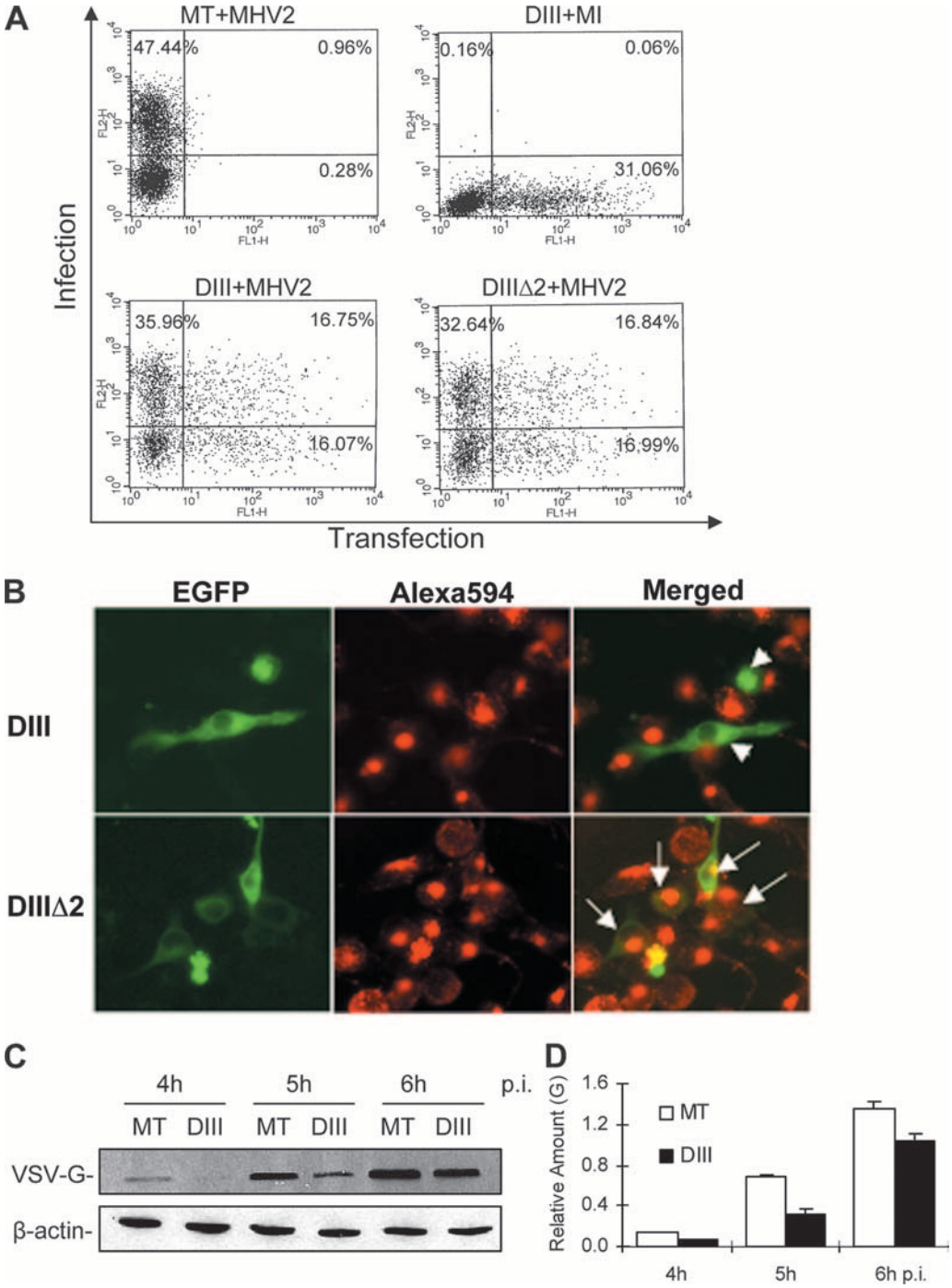

FIG. 7. Overexpression of a dominant-negative mutant of Eps15 could not prevent MHV-2 infection. (A) Effect of dominant-negative Eps15 on MHV-2 infection. DBT cells were transfected with an Eps15 dominant-negative mutant, EGFP-DIII (DIII), or a control, EGFP-DIIIΔ2 (DIIIΔ2), which exhibits a similar effect on endocytosis to that of the wild-type Eps15, or mock transfected (MT). At 24 h posttransfection, cells were either infected with MHV-2 at an MOI of 10 or mock-infected (MI). At 6 h p.i., cells were fixed and stained for the viral N protein using an N-specific monoclonal antibody and PE conjugate. Flow cytometric analysis was used to quantify the expression of the EGFP (green) and viral N protein (red), which monitors the transfection (*x* axis) and infection (*y* axis), respectively. The percentage of cells within each quadrant is shown. Data were representative of three independent experiments. (B) Expression of dominant-negative Eps15 blocked transferrin uptake. DBT cells grown on glass coverslips were transiently transfected with either EGFP-DIII (DIII) or EGFP-DIIIΔ2 (DIIIΔ2) for 24 h. Alexa 594-labeled transferrin was bound to serum-starved cells for 20 min at 4°C. Cells were washed, transferred to 37°C for 15 min, washed with low-pH glycine to remove uninternalized ligand, and fixed. Cells were then observed under a dual-fluorescence microscope. The images were taken with an AxioCam MRc color camera using AvioVision software. White arrowheads in the upper right panel indicate that the EGFP-expressing cells (green) failed to take up transferrin (red), whereas the arrows in the lower right panel indicate the cells both expressing EGFP (green) and taking up transferrin (red). (C) Expression of dominant-negative Eps15 inhibited VSV gene expression. EGFP-DIII-transfected (DIII) or mock-transfected (MT) DBT cells were infected with VSV at an MOI of 10. Viral G protein expression was detected by Western blotting at various time points p.i., as indicated. β-Actin was used as an internal control. (D) Quantification of the protein bands shown in panel C. The amount of the G protein was quantified by densitometric analysis with UPV software, normalized with β-actin expressed in virus-infected cells, and presented as the mean relative amount. Error bars indicate the standard deviations of the means. Data are representative of three independent experiments.

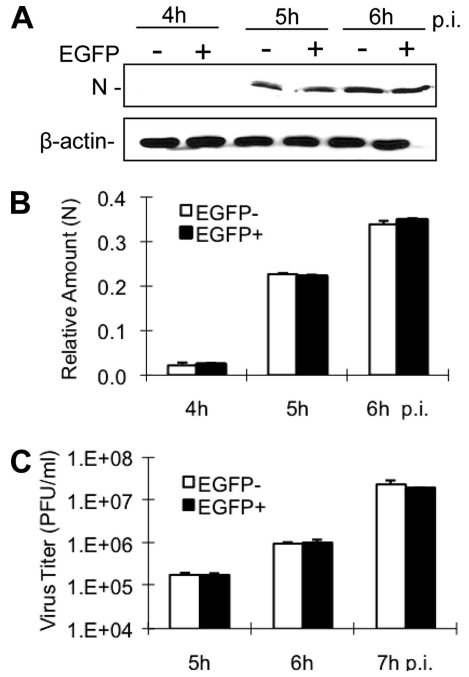

FIG. 8. MHV-2 gene expression and propagation were unaffected by the expression of the dominant-negative mutant of Eps15. DBT cells were transfected with the dominant-negative mutant of Eps15, EGFP-DIII. At 24 h posttransfection, DBT cells were subjected to FACS to separate EGFP-positive (+) and EGFP-negative (−) cell populations, which were then separately infected with MHV-2 at an MOI of 10. (A) Expression of the viral N protein was detected by Western blot analysis, with β-actin as an internal control. (B) Quantification of the protein bands shown in panel A. The amounts of the N protein were quantified by densitometric analysis and normalized with β-actin. (C) Titers of virus were determined at the indicated time points p.i. by plaque assay in triplicate and expressed as mean PFU/ml. Error bars indicate the standard deviations of the means. All data are representative of at least three independent experiments.

world may have different properties with respect to cell entry. Although the original source of the MHV-A59 strain may be the same, mutations likely have occurred during subsequent propagation and adaptation in various types of cell cultures in different laboratories over the years. Indeed, MHV-A59 mutants that have arisen during prolonged cell cultures have acquired an ability to enter cells derived from different animal species (3). The MHV-JHM (MHV-4) mutant, OBLV60, which is isolated from mouse neuronal cell culture (OBL20) following continuous propagation, becomes sensitive to lysosomotropic agents, as opposed to its parental virus, whose entry into DBT cells is insensitive to lysosomotropic agents (20). This phenotypic change has been attributed to mutations of several amino acids in the spike protein of OBLV60 (20). In addition, a single amino acid mutation in the spike protein of recombinant RA59/MHV-2S_{S757R} effectively reverses the sensitivity of the parental viruses to lysosomotropic agents (51). Thus, it will be interesting to directly compare the MHV-A59 viruses from these different laboratories and to identify their potential differences in amino acid sequences of the spike proteins.

The molecular events leading to MHV-2 entry via clathrin-mediated endocytosis are further characterized in this study. As found in other viral systems, such as human polyomavirus JC virus, Sindbis virus, and VSV, pH-dependent clathrin-mediated endocytosis is dependent on the regulatory (or accessory) protein Eps15 (52, 63). Although the exact role of Eps15 in clathrin-mediated endocytosis is not clear, previous studies have shown that Eps15 is highly conserved among species during evolution and that Eps15 is ubiquitously expressed and is associated with AP-2 (6). Disruption of its function by either microinjection of anti-Eps15 antibody or overexpression of the dominant-negative mutants interfered with transferrin and EGFR internalization in many types of cells (6). Indeed, overexpression of the dominant-negative mutant of Eps15 (DIII) in DBT cells blocked the uptake of transferrin (Fig. 7B), which enters cells via Eps15-dependent, clathrin-mediated endocytosis (63). In addition, overexpression of DIII inhibited VSV infection in DBT cells (Fig. 7C and D). This finding is consistent with those in a previous report, which show that VSV infection was inhibited by chlorpromazine treatment, clathrin knockdown with siRNA, and expression of dominant-negative mutant of Eps15 (63). Unexpectedly, however, the overexpression of DIII in DBT cells did not affect MHV-2 infection, as measured by both viral gene expression and titers of virus (Fig. 7A and 8). We showed that there was no difference in the number and mean fluorescence intensity of the virus-infected cells that were either transfected with EGFP-DIII or the control, EGFP-DIIIΔ2 (Fig. 7A). Furthermore, viral gene expression and viral titers were similar in EGFP-DIII-expressing and -nonexpressing cells following FACS (Fig. 8), thus demonstrating that Eps15 is not essential for MHV-2 entry into DBT cells. It should be noted that although influenza A virus enters MDCK, BHK, and Mv1 lung cells via clathrin-mediated endocytosis (36, 54), its entry into HeLa cells is independent of clathrin and Eps15, since its infection in HeLa cells was not inhibited by expression of dominant-negative Eps15 and by treatment with chlorpromazine and potassium depletion, the latter of which also blocks clathrin-mediated endocytosis (58). Likewise, entry of SARS-CoV into HepG2 and COS7 cells requires clathrin (25), while its entry into Vero E6 cells is independent of clathrin and Eps15 (69). Thus, to our knowledge, MHV-2 is the first virus that enters DBT cells through pH-dependent, clathrin-mediated endocytosis but is independent of Eps15.

Our findings suggest that clathrin-mediated endocytosis may be regulated by multiple accessory proteins at multiple steps during the transport of ligand/receptor cargos from the cell surface to the endosomes. Some of these proteins may be functionally redundant, while others have distinct functions. For example, clathrin-mediated MHV-2 entry may involve multiple redundant proteins, such that depletion of one of the proteins, such as Eps15, would not significantly affect its entry. In support of this interpretation are the findings that EGFR and transferrin endocytosis proceeded even when the expression of several accessory proteins was knocked down individually, but it was severely impaired when they were depleted simultaneously (23). Our findings may also suggest that the selection or recruitment of these accessory proteins into the "shipping vesicle" is determined by the ligand and/or receptor itself. It is possible that the cytoplasmic tail of a receptor molecule has a specific internalization signal that recognizes the AP-2 adaptor (28), which in turn bridges the receptor to

clathrin for internalization. It has been shown that EGFR is endocytosed through a clathrin-mediated pathway in response to its ligand binding. The EGFR intrinsic tyrosine kinase activity results in the phosphorylation of a large number of cellular molecules to facilitate the intracellular transport of EGFR (30). Eps15 is also site-specifically phosphorylated by EGFR, and this phosphorylation is absolutely required for its function in endocytosis (11, 18). However, phosphorylation of Eps15 is not absolutely required for endocytosis of other receptors, as in the case of constitutive endocytosis of transferrin receptor (11). Likewise, the keratinocyte growth factor receptor was endocytosed through the clathrin pathway independently of Eps15 phosphorylation and recruitment to the membrane (5). These data indicate that the selection and requirement for the phosphorylation of the accessory proteins can be determined by the ligands and/or receptors being endocytosed. This may explain why the three enveloped viruses (Sindbis virus, VSV, and MHV-2), which utilize different types of receptors, have different requirements for Eps15, although they all enter cells via clathrin-mediated endocytosis. Presumably, the binding of the MHV-2 spike protein to the CEACAM1 receptor triggers cascades of signals that are distinct from those triggered by VSV glycoprotein (G) receptor binding. In this regard, MHV-2 may provide an ideal tool for identifying novel accessory proteins in the clathrin-mediated endocytic pathway that is independent of Eps15.

ACKNOWLEDGMENTS

We thank the following individuals for their generosity in providing the reagents that were essential for accomplishing this study: A. Benmerah and A. Dautry-Varsat (Institut Pasteur, Paris, France) for the Eps15 constructs, M. Chow (UAMS) for the caveolin constructs, M. Chow and M. Whitt (University of Tennessee Medical School, Memphis, TN) for VSV and anti-VSV G antibody, S. Stohlman (The Cleveland Clinic, Cleveland, OH) and J. Fleming (University of Wisconsin, Madison, WI) for the monoclonal antibody to the MHV N protein, and M. Lai (University of Southern California Keck School of Medicine, Los Angeles, CA) for MHV-2 and MHV-A59.

This work was supported by Public Health Service grant NS047499 and in part by the P30 core grant NS047546 and grant AI061204 from the National Institutes of Health.

REFERENCES

1. **Anderson, H. A., Y. Chen, and L. C. Norkin.** 1996. Bound simian virus 40 translocates to caveolin-enriched membrane domains, and its entry is inhibited by drugs that selectively disrupt caveolae. Mol. Biol. Cell **7:**1825–1834.
2. **Anderson, R. G. W.** 1998. The caveolae membrane system. Annu. Rev. Biochem. **67:**199–225.
3. **Baric, R. S., E. Sullivan, L. Hensley, B. Yount, and W. Chen.** 1999. Persistent infection promotes cross-species transmissibility of mouse hepatitis virus. J. Virol. **73:**638–649.
4. **Bavari, S., C. M. Bosio, E. Wiegand, G. Ruthel, A. B. Will, T. W. Geisbert, M. Hevey, C. Schmaljohn, A. Schmaljohn, and M. J. Aman.** 2002. Lipid raft microdomains: a gateway for compartmentalized trafficking of Ebola and Marburg viruses. J. Exp. Med. **195:**593–602.
5. **Belleudi, F., V. Visco, M. Ceridono, L. Leone, R. Muraro, L. Frati, and M. R. Torrisi.** 2003. Ligand-induced clathrin-mediated endocytosis of the keratinocyte growth factor receptor occurs independently of either phosphorylation or recruitment of eps15. FEBS Lett. **553:**262–270.
6. **Benmerah, A., J. Gagnon, B. Bègue, B. Mégarbané, A. Dautry-Varsat, and N. Cerf-Bensussan.** 1995. The tyrosine kinase substrate Eps15 is constitutively associated with the plasma membrane adaptor AP-2. J. Cell Biol. **131:**1831–1838.
7. **Benmerah, A., V. Poupon, N. Cerf-Bensussan Dautry, and A. Varsat.** 2000. Mapping of Eps15 domains involved in its targeting to clathrin-coated pits. J. Biol. Chem. **275:**3288–3295.
8. **Brown, D. A., and E. London.** 1998. Functions of lipid rafts in biological membranes. Annu. Rev. Cell Dev. Biol. **14:**111–136.
9. **Carbone, R., S. Fre, G. Iannolo, F. Belleudi, P. Mancini, P. G. Pelicci, M. R. Torrisi, and P. P. Di Fiore.** 1997. Eps15 and Eps15R are essential components of the endocytic pathway. Cancer Res. **57:**5498–5504.
10. **Chazal, N., and D. Gerlier.** 2003. Virus entry, assembly, budding, and membrane rafts. Microbiol. Mol. Biol. Rev. **67:**226–237.
11. **Confalonieri, S., A. Salcini, E. C. Puri, C. Tacchetti, and P. P. Di Fiore.** 2000. Tyrosine phosphorylation of Eps15 is required for ligand-regulated, but not constitutive, endocytosis. J. Cell Biol. **150:**905–912.
12. **de Haan, C. A., K. Stadler, G. J. Godeke, B. J. Bosch, and P. J. Rottier.** 2004. Cleavage inhibition of the murine coronavirus spike protein by a furin-like enzyme affects cell-cell but not virus-cell fusion. J. Virol. **78:**6048–6054.
13. **Duncan, M. J., J. S. Shin, and S. N. Abraham.** 2002. Microbial entry through caveolae: variations on a theme. Cell Microbiol. **4:**783–791.
14. **Durrbach, A., D. Louvard, and E. Coudrier.** 1996. Actin filaments facilitate two steps of endocytosis. J. Cell Sci. **109:**457–465.
15. **Eifart, P., K. Ludwig, C. Böttcher, C. A. de Haan, P. J. Rottier, T. Korte, and A. Herrmann.** 2007. Role of endocytosis and low pH in murine hepatitis virus strain A59 cell entry. J. Virol. **81:**10758–10768.
16. **Empig, C. J., and M. A. Goldsmith.** 2002. Association of the caveola vesicular system with cellular entry by filoviruses. J. Virol. **76:**5266–5270.
17. **Farsad, K., and P. De Camilli.** 2003. Mechanisms of membrane deformation. Curr. Opin. Cell Biol. **15:**372–381.
18. **Fazioli, F., L. Minichiello, B. Matoskova, W. T. Wong, and P. P. Di Fiore.** 1993. Eps 15, a novel tyrosine kinase substrate, exhibits transforming activity. Mol. Cell. Biol. **13:**5814–5828.
19. **Frana, M. F., J. N. Behnke, L. S. Sturman, and K. V. Holmes.** 1985. Proteolytic cleavage of the E2 glycoprotein of murine coronavirus: host-dependent differences in proteolytic cleavage and cell fusion. J. Virol. **56:**912–920.
20. **Gallagher, T. M., C. Escarmis, and M. J. Buchmeier.** 1991. Alteration of the pH dependence of coronavirus-induced cell fusion: effect of mutations in the spike glycoprotein. J. Virol. **65:**1916–1928.
21. **Heuser, J. E., and R. G. Anderson.** 1989. Hypertonic media inhibit receptor-mediated endocytosis by blocking clathrin-coated pit formation. J. Cell Biol. **108:**389–400.
22. **Hirano, N., K. Fujiwara, S. Hino, and M. Matumoto.** 1974. Replication and plaque formation of mouse hepatitis virus (MHV-2) in mouse cell line DBT culture. Arch. Gesamte Virusforsch. **44:**298–302.
23. **Huang, F., A. Khvorova, W. Marshall, and A. Sorkin.** 2004. Analysis of clathrin-mediated endocytosis of epidermal growth factor receptor by RNA interference. J. Biol. Chem. **279:**16657–16661.
24. **Hugon, J. S., G. Bennett, P. Pothier, and Z. Ngoma.** 1987. Loss of microtubules and alteration of glycoprotein migration in organ cultures of mouse intestine exposed to nocodazole or colchicine. Cell Tissue Res. **248:**653–662.
25. **Inoue, Y., N. Tanaka, Y. Tanaka, S. Inoue, K. Morita, M. Zhuang, T. Hattori, and K. Sugamura.** 2007. Clathrin-dependent entry of severe acute respiratory syndrome coronavirus into target cells expressing ACE2 with the cytoplasmic tail deleted. J. Virol. **81:**8722–8729.
26. **Keen, J. H.** 1990. Clathrin and associated assembly and disassembly proteins. Annu. Rev. Biochem. **59:**415–438.
27. **Kirchhausen, T.** 1999. Adaptors for clathrin-mediated traffic. Annu. Rev. Cell Dev. Biol. **15:**705–732.
28. **Kirchhausen, T.** 2002. Clathrin adaptors really adapt. Cell **109:**413–416.
29. **Kurzchalia, T. V., P. Dupree, and S. Monier.** 1994. VIP21-Caveolin, a protein of the trans-Golgi network and caveolae. FEBS Lett. **346:**88–91.
30. **Lamaze, C., and S. L. Schmid.** 1995. Recruitment of epidermal growth factor receptors into coated pits requires their activated tyrosine kinase. J. Cell Biol. **129:**47–54.
31. **Lamaze, C., L. M. Fujimoto, H. L. Yin, and S. L. Schmid.** 1997. The actin cytoskeleton is required for receptor-mediated endocytosis in mammalian cells. J. Biol. Chem. **272:**20332–20335.
32. **Le, P. U., and I. R. Nabi.** 2003. Distinct caveolae-mediated endocytic pathways target the Golgi apparatus and the endoplasmic reticulum. J. Cell Sci. **116:**1059–1071.
33. **Liao, Z., L. M. Cimakasky, R. Hampton, D. H. Nguyen, and J. E. Hildreth.** 2001. Lipid rafts and HIV pathogenesis: host membrane cholesterol is required for infection by HIV type 1. AIDS Res. Hum. Retrovir. **17:**1009–1019.
34. **Lu, X., and J. Silver.** 2000. Ecotropic murine leukemia virus receptor is physically associated with caveolin and membrane rafts. Virology **276:**251–258.
35. **Marsh, M., and A. Helenius.** 1980. Adsorptive endocytosis of Semliki Forest virus. J. Mol. Biol. **142:**439–454.
36. **Matlin, K. S., H. Reggio, A. Helenius, and K. Simons.** 1981. Infectious entry pathway of influenza virus in a canine kidney cell line. J. Cell Biol. **91:**601–613.
37. **Matlin, K. S., H. Reggio, A. Helenius, and K. Simons.** 1982. Pathway of vesicular stomatitis virus entry leading to infection. J. Mol. Biol. **156:**609–631.
38. **Meier, O., K. Boucke, S. V. Hammer, S. Keller, R. P. Stidwill, S. Hemmi, and U. F. Greber.** 2002. Adenovirus triggers macropinocytosis and endosomal leakage together with its clathrin-mediated uptake. J. Cell Biol. **158:**1119–1131.
39. **Merrifield, C. J., M. E. Feldman, L. Wan, and W. Almers.** 2002. Imaging

actin and dynamin recruitment during invagination of single clathrin-coated pits. Nat. Cell Biol. **4:**691–698.
40. **Miranda, A. F., G. C. Godman, A. D. Deitch, and S. W. Tanenbaum.** 1974. Action of cytochalasin D on cells of established lines. I. Early events. J. Cell Biol. **61:**481–500.
41. **Misinzo, G., P. Meerts, M. Bublot, J. Mast, H. M. Weingartl, and H. J. Nauwynck.** 2005. Binding and entry characteristics of porcine circovirus 2 in cells of the porcine monocytic line 3D4/31. J. Gen. Virol. **86:**2057–2068.
42. **Mora, R., V. L. Bonilha, A. Marmorstein, P. E. Scherer, D. Brown, M. P. Lisanti, and E. Rodriguez-Boulan.** 1999. Caveolin-2 localizes to the Golgi complex but redistributes to plasma membrane, caveolae, and rafts when co-expressed with caveolin-1. J. Biol. Chem. **74:**25708–25717.
43. **Nomura, R., A. Kiyota, E. Suzaki, K. Kataoka, Y. Ohe, K. Miyamoto, T. Senda, and T. Fujimoto.** 2004. Human coronavirus 229E binds to CD13 in rafts and enters the cell through caveolae. J. Virol. **78:**8701–8708.
44. **Park, D. S., S. E. Woodman, W. Schubert, A. W. Cohen, P. G. Frank, M. Chandra, J. Shirani, B. Razani, B. Tang, L. A. Jelicks, S. M. Factor, L. M. Weiss, H. B. Tanowitz, and M. P. Lisanti.** 2002. Caveolin-1/3 double-knockout mice are viable, but lack both muscle and non-muscle caveolae, and develop a severe cardiomyopathic phenotype. Am. J. Pathol. **160:**2207–2217.
45. **Parolini, I., M. Sargiacomo, F. Galbiati, G. Rizzo, F. Grignani, J. A. Engelman, T. Okamoto, T. Ikezu, P. E. Scherer, R. Mora, E. Rodriguez-Boulan, C. Peschle, and M. P. Lisanti.** 1999. Expression of caveolin-1 is required for the transport of caveolin-2 to the plasma membrane. Retention of caveolin-2 at the level of the Golgi complex. J. Biol. Chem. **274:**25718–25725.
46. **Parton, R. G., B. Joggerst, and K. Simons.** 1994. Regulated internalization of caveolae. J. Cell Biol. **127:**1199–1215.
47. **Pelkmans, L., J. Kartenbeck, and, A. Helenius.** 2001. Caveolar endocytosis of simian virus 40 reveals a new two-step vesicular-transport pathway to the ER. Nat. Cell Biol. **3:**473–483.
48. **Pelkmans, L., D. Puntener, and A. Helenius.** 2002. Local actin polymerization and dynamin recruitment in SV40-induced internalization of caveolae. Science **296:**535–539.
49. **Pelkmans, L., and A. Helenius.** 2003. Insider information: what viruses tell us about endocytosis. Curr. Opin. Cell Biol. **15:**414–422.
50. **Pickl, W. F., F. X. Pimentel-Muinos, and B. Seed.** 2001. Lipid rafts and pseudotyping. J. Virol. **75:**7175–7183.
51. **Qiu, Z., S. T. Hingley, G. Simmons, C. Yu, J. Das Sarma, P. Bates, and S. R. Weiss.** 2006. Endosomal proteolysis by cathepsins is necessary for murine coronavirus mouse hepatitis virus type 2 spike-mediated entry. J. Virol. **80:**5768–5776.
52. **Querbes, W., A. Benmerah, D. Tosoni, P. P. Di Fiore, and W. J. Atwood.** 2004. A JC virus-induced signal is required for infection of glial cells by a clathrin- and Eps15-dependent pathway. J. Virol. **78:**250–256.
53. **Rothberg, K. G., J. E. Heuser, W. C. Donzell, Y. S. Ying, J. R. Glenney, and R. G. Anderson.** 1992. Caveolin, a protein component of caveolae membrane coats. Cell **68:**673–682.
54. **Roy, A.-M. M., J. S. Parker, C. R. Parrish, and G. R. Whittaker.** 2000. Early stages of influenza virus entry into Mv-1 lung cells: involvement of dynamin. Virology **267:**17–28.
55. **Salcini, A. E., S. Confalonierie, M. Doria, E. Santolini, E. Tassi, O. Minenkova, G. Cesareni, P. G. Pelicci, and P. P. Di Fiore.** 1997. Binding specificity and in vivo targets of the EH domain, a novel protein-protein interaction module. Genes Dev. **11:**2239–2249.
56. **Scheiffele, P., M. G. Roth, and K. Simons.** 1997. Interaction of influenza virus hemagglutinin with sphingolipid-cholesterol membrane domains via its transmembrane domain. EMBO J. **16:**5501–5508.
57. **Scherer, P. E., T. Okamoto, M. Chun, I. Nishimoto, H. F. Lodish, and M. P. Lisanti.** 1996. Identification, sequence, and expression of caveolin-2 define a caveolin gene family. Proc. Natl. Acad. Sci. USA **93:**131–135.
58. **Sieczkarski, S. B., and G. R. Whittaker.** 2002. Influenza virus can enter and infect cells in the absence of clathrin-mediated endocytosis. J. Virol. **76:**10455–10464.
59. **Simmons, G., D. N. Gosalia, A. J. Rennekamp, J. D. Reeves, S. L. Diamond, and P. Bates.** 2005. Inhibitors of cathepsin L prevent severe acute respiratory syndrome coronavirus entry. Proc. Natl. Acad. Sci. USA **102:**11876–11881.
60. **Stan, R. V.** 2005. Structure of caveolae. Biochim. Biophys. Acta **1746:**334–348.
61. **Stohlman, S. A., and M. M. Lai.** 1979. Phosphoproteins of mouse hepatitis virus. J. Virol. **32:**672–675.
62. **Subtil, A., A. Hemar, and A. Dautry-Varsat.** 1994. Rapid endocytosis of interleukin 2 receptors when clathrin-coated pit endocytosis is inhibited. J. Cell Sci. **107:**3461–3468.
63. **Sun, X., V. K. Yau, B. J. Briggs, and G. R. Whittaker.** 2005. Role of clathrin-mediated endocytosis during vesicular stomatitis virus entry into host cells. Virology **338:**53–60.
64. **Tang, Z., P. E. Scherer, T. Okamoto, K. Song, C. Chu, D. S. Kohtz, I. Nishimoto, H. F. Lodish, and M. P. Lisanti.** 1996. Molecular cloning of caveolin-3, a novel member of the caveolin gene family expressed predominantly in muscle. J. Biol. Chem. **271:**2255–2261.
65. **Tebar, F., T. Sorkina, A. S. Sorkin, M. Ericsson, and T. Kirchhausen.** 1996. Eps15 is a component of clathrin-coated pits and vesicles and is located at the rim of coated pits. J. Biol. Chem. **271:**28727–28730.
66. **Thomsen, P., K. Roepstorff, M. Stahlhut, and B. van Deurs.** 2002. Caveolae are highly immobile plasma membrane microdomains, which are not involved in constitutive endocytic trafficking. Mol. Biol. Cell **13:**238–250.
67. **van Deurs, B., F. von Bulow, P. K. Vilhardt, K. Holm, and K. Sandvig.** 1996. Destabilization of plasma membrane structure by prevention of actin polymerization. Microtubule-dependent tabulation of the plasma membrane. J. Cell Sci. **109:**1655–1665.
68. **Wakeham, D. E., L. Abi-Rached, M. C. Towler, J. D. Wilbur, P. Parham, and F. M. Brodsky.** 2005. Clathrin heavy and light chain isoforms originated by independent mechanisms of gene duplication during chordate evolution. Proc. Natl. Acad. Sci. USA **102:**7209–7214.
69. **Wang, H., P. Yang, K. Liu, F. Guo, Y. Zhang, G. Zhang, and C. Jiang.** 2008. SARS coronavirus entry into host cells through a novel clathrin- and caveolae-independent endocytic pathway. Cell Res. **18:**290–301.
70. **Wang, L. H., K. G. Rothberg, and R. G. Anderson.** 1993. Mis-assembly of clathrin lattices on endosomes reveals a regulatory switch for coated pit formation. J. Cell Biol. **123:**1107–1117.
71. **Williams, R. K., G. S. Jiang, and K. V. Holmes.** 1991. Receptor for mouse hepatitis virus is a member of the carcinoembryonic antigen family of glycoproteins. Proc. Natl. Acad. Sci. USA **88:**5533–5536.
72. **Yarar, D., C. M. Waterman-Storer, and S. L. Schmid.** 2005. A dynamic actin cytoskeleton functions at multiple stages of clathrin-mediated endocytosis. Mol. Biol. Cell **16:**964–975.
73. **Yokomori, K., N. La Monica, S. Makino, C. K. Shieh, and M. M. Lai.** 1989. Biosynthesis, structure, and biological activities of envelope protein gp65 of murine coronavirus. Virology **173:**683–691.
74. **Zhang, X., D. R. Hinton, S. Park, B. Parra, C. L. Liao, M. M. Lai, and S. A. Stohlman.** 1998. Expression of hemagglutinin/esterase by a mouse hepatitis virus coronavirus defective-interfering RNA alters viral pathogenesis. Virology **242:**170–183.